



Brazilian Journal of Physics

ISSN: 0103-9733

luizno.bjp@gmail.com

Sociedade Brasileira de Física

Brasil

Hossen, M. R.; Mamun, A. A.
Electrostatic Solitary Structures in a Relativistic Degenerate Multispecies Plasma
Brazilian Journal of Physics, vol. 44, núm. 6, 2014, pp. 673-681
Sociedade Brasileira de Física
São Paulo, Brasil

Available in: <http://www.redalyc.org/articulo.oa?id=46432477010>

- How to cite
- Complete issue
- More information about this article
- Journal's homepage in redalyc.org

redalyc.org

Scientific Information System
Network of Scientific Journals from Latin America, the Caribbean, Spain and Portugal
Non-profit academic project, developed under the open access initiative

Electrostatic Solitary Structures in a Relativistic Degenerate Multispecies Plasma

M. R. Hossen · A. A. Mamun

Received: 17 July 2014 / Published online: 30 August 2014
© Sociedade Brasileira de Física 2014

Abstract The nonlinear propagation of cylindrical and spherical modified ion-acoustic (mIA) waves in an unmagnetized, collisionless, relativistic, degenerate multispecies plasma has been investigated theoretically. This plasma system is assumed to contain both relativistic degenerate electron and positron fluids, nonrelativistic degenerate positive and negative ions, and positively charged static heavy ions. The restoring force is provided by the degenerate pressures of the electrons and positrons, whereas the inertia is provided by the mass of positive and negative ions. The positively charged static heavy ions participate only in maintaining the quasi-neutrality condition at equilibrium. The nonplanar K-dV and mK-dV equations are derived by using reductive perturbation technique and numerically analyzed to identify the basic features (speed, amplitude, width, etc.) of mIA solitary structures. The basic characteristics of mIA solitary waves are found to be significantly modified by the effects of degenerate pressures of electron, positron, and ion fluids, their number densities, and various charge states of heavy ions. The implications of our results to dense plasmas in astrophysical compact objects (e.g., nonrotating white dwarfs, neutron stars, etc.) are briefly mentioned.

Keywords Solitary structures · Degenerate pressure · Nonplanar geometry · Relativistic effect · Compact objects

1 Introduction

Recently, electron-positron plasmas have received a great deal of attention because of their importance not only in plasma astrophysics (i.e., in early universe, in active galactic nuclei) [1, 2] but also in laboratory devices [3]. In fact, positrons are created in the interstellar medium when the atoms interact with the cosmic ray nuclei [4]. The annihilation, which takes place in the interaction of matter (electrons) and antimatter (positrons), usually occurs at much longer characteristic time scales compared with the time in which the collective interaction between the charged particles takes place [5]. Electron-positron plasmas are created in the presence of strong electric or magnetic fields or extremely high temperatures, where massive pair production sets in. The ultradense electron-positron plasmas with ions are believed to be found in compact astrophysical bodies like white dwarfs, neutron stars, black holes, etc. as well as in intense laser-matter interaction experiments [6–8]. The multi-ion plasma is one of the most fascinating aspects of nonlinear phenomena in modern plasma physics research. Ionosphere and magnetosphere of Earth, solar wind, bow shock in front of the magnetopause boundary layers, heliosphere, Saturn's magnetosphere, coma of comet Halley, neutral beam sources, plasma processing reactors, low-temperature laboratory experiments, and the existence of multi-ion (both positive-negative ion) plasmas have been found [9–16].

In present days, there has been a great deal of interest in understanding the basic properties of matter under extreme conditions [17–19, 21]. White dwarf is an example of matter under extreme condition. The basic constituents of white dwarfs are mainly oxygen, carbon, and helium with an envelope of hydrogen gas. In some relatively massive white dwarfs, one can think of the presence of heavier elements

M. R. Hossen (✉) · A. A. Mamun
Department of Physics, Jahangirnagar University,
Savar, Dhaka 1342, Bangladesh
e-mail: rasel.plasma@gmail.com

like iron within the stars. The existence of heavy elements is found to form in a prestellar stage of the evolution of the universe, when all matter was compressed to extremely high densities and possessed correspondingly high temperatures [22]. Thus, the ionized condition within the massive compact stars occurs due to this high density and temperature. In case of such a compact object, the degenerate electron number density is so high (in white dwarfs it can be of the order of 10^{30} cm^{-3} , even more [23–25]) that the electron Fermi energy is comparable to the electron mass energy and the electron speed is comparable to the speed of light in a vacuum. In many space plasma phenomena, heavy ions are present in abundance which is not negligible relative to the protons. In some relatively massive white dwarfs, one can think of the presence of heavier elements like iron within the stars. For such interstellar compact objects, the equation of state for degenerate ions and electrons is mathematically explained by Chandrasekhar [19] for two limits, named as nonrelativistic and ultrarelativistic limits. Chandrasekhar [17, 19] presented a general expression for the relativistic ion and electron pressures in his classical papers. The pressure for ion fluid can be given by the following equation:

$$P_i = K_i n_i^\alpha, \quad (1)$$

where

$$\alpha = \frac{5}{3}; \quad K_i = \frac{3}{5} \left(\frac{\pi}{3} \right)^{\frac{1}{3}} \frac{\pi \hbar^2}{m} \simeq \frac{3}{5} \Lambda_c \hbar c, \quad (2)$$

for the nonrelativistic limit (where $\Lambda_c = \pi \hbar / mc = 1.2 \times 10^{-10} \text{ cm}$, and \hbar is the Planck constant divided by 2π). While for the electron fluid,

$$P_e = K_e n_e^\gamma, \quad (3)$$

and while for the positron fluid

$$P_p = K_p n_p^\gamma, \quad (4)$$

where for nonrelativistic limit [17–19, 23, 24]

$$\gamma = \alpha = \frac{5}{3}; \quad K_e = K_p = K_i \quad (5)$$

and for the ultrarelativistic limit [17–19, 23, 24]

$$\gamma = \frac{4}{3}; \quad K_e = K_p = \frac{3}{4} \left(\frac{\pi^2}{9} \right)^{\frac{1}{3}} \hbar c \simeq \frac{3}{4} \hbar c. \quad (6)$$

Studies of nonlinear wave phenomena in collisionless multispecies plasmas have received an enormous attention in understanding the localized electrostatic disturbances in astrophysical environments and laboratory plasma systems. Khan and Arshad [26] considered an unmagnetized, ultra-dense plasma containing degenerate Fermi gas of electrons and positrons, and classical ion gas and reported that the effect of ion temperature, positron concentration, disper-

sion and dissipation significantly modify the solitary and shock structures. Germin et al. [27] worked on an adiabatic electron-positron plasma and experimentally found that the electron and positron peaks may be separated by large distances, found no completely isolated soliton like structures. Zeba et al. [28] also considered a warm collisionless electron-positron-ion plasma with ultrarelativistic degenerate electrons and positrons and studied the existence regions for ion solitary pulses. Roy et al. [29] considered an electron-positron-ion plasma and rigorously investigated the basic features of solitary waves and double layers. Since, the dense astrophysical quantum plasmas can be confined by stationary heavy ions. Therefore, the effect of the heavy ions has to be taken into account, especially for astrophysical observations (such as white dwarfs, neutron stars, black holes etc) where the degenerate plasma pressure and heavy ions play an important role in the formation and stability of the existing waves. Zobaer et al. [30, 31] considered an electron-positron plasma containing nonrelativistic ion fluids and both nonrelativistic and ultrarelativistic electron fluids, and theoretically observed the basic features of solitary and double-layer structures. All of the authors did not consider the effect of heavy ions and their different charging situations which can significantly modify the propagation of solitary and shock structures. To the best of our knowledge, the mIA waves in such considerable plasma system has never been addressed. Therefore, it is worthwhile to present a first study for the mIA solitary waves where degenerate plasma pressure, nonplanar geometry, various charging states of positively charged heavy ions play a vital role.

2 Governing Equations

We consider an unmagnetized, collisionless degenerate multispecies plasma system consisting of nonrelativistic cold degenerate positive and negative ion fluids, both nonrelativistic and ultra-relativistic degenerate electron and positron fluids, and positively charged static heavy ions. Thus, at equilibrium, we have $Z_{pi}n_{pi0} + Z_h n_{h0} + n_{p0} = n_{e0} + Z_{ni}n_{ni0}$. We also consider the equal number density of positive and negative ions, i.e., $n_{pi0} = n_{ni0}$, and electron and positron, i.e., $n_{p0} = n_{e0}$, at equilibrium. The nonlinear dynamics of the electrostatic waves propagating in such a degenerate multispecies plasma system is governed by the following normalized equations:

$$\frac{\partial n_s}{\partial t} + \frac{1}{r^\nu} \frac{\partial}{\partial r} (r^\nu n_s u_s) = 0, \quad (7)$$

$$\frac{\partial u_{pi}}{\partial t} + u_{pi} \frac{\partial u_{pi}}{\partial r} + \frac{\partial \phi}{\partial r} + \frac{K_1}{n_{pi}} \frac{\partial n_{pi}^\alpha}{\partial r} = 0, \quad (8)$$

$$\frac{\partial u_{ni}}{\partial t} + u_{ni} \frac{\partial u_{ni}}{\partial r} - \beta \frac{\partial \phi}{\partial r} + \frac{K_1}{n_{ni}} \frac{\partial n_{ni}^\alpha}{\partial r} = 0, \quad (9)$$

$$n_e \frac{\partial \phi}{\partial r} - K_2 \frac{\partial n_e^\gamma}{\partial r} = 0, \quad (10)$$

$$n_p \frac{\partial \phi}{\partial r} - K_2 \frac{\partial n_p^\gamma}{\partial r} = 0, \quad (11)$$

$$\frac{1}{r^\nu} \frac{\partial}{\partial r} \left(r^\nu \frac{\partial \phi}{\partial r} \right) = \alpha_e n_e - n_{pi} + \alpha_n n_{ni} - \alpha_p n_p - Z_h \mu_h, \quad (12)$$

where n_s is the plasma number density of the species s ($s = e$ for electron, pi for positive ion, ni for negative ion, and p for positron) normalized by its equilibrium value n_{pi0} ; u_s is the plasma species fluid speed normalized by $C_{im} = (m_e c^2 / m_i)^{1/2}$ with m_e (m_i) being the electron (ion) rest mass and c being the speed of light in vacuum; ϕ is the electrostatic wave potential normalized by $m_e c^2 / e$ with e being the magnitude of the charge of an electron; the time variable (t) is normalized by $\omega_{pi} = (4\pi n_{i0} e^2 / m_i)^{1/2}$; and the space variable (r) is normalized by $\lambda_m = (m_e c^2 / 4\pi n_{s0} e^2)^{1/2}$. Here, $\alpha_e (= n_{e0} / Z_{pi} n_{pi0})$ is the ratio of the number density of electron and positive ion multiplied by charge per positive ion Z_{pi} ; $\alpha_n (= Z_{ni} n_{e0} / Z_{pi} n_{pi0})$ is the ratio of number density of electron and positive ions multiplied by their charge per ion, Z_s (where $s = pi, ni$); $\alpha_p (= n_{p0} / Z_{pi} n_{pi0})$ is the ratio of number density of positron and positive ions multiplied by their charge per positive ion Z_{pi} ; β is the ratio of the number density of negative and positive ions multiplied by their charge per ion, Z_s (where $s = pi, ni$); and $\mu_h (= n_{h0} / Z_{pi} n_{pi0})$ is the ratio of the number density of positively charged heavy ions and positive ions multiplied by their charge per positive ion, Z_{pi} . It is needed here to note that $\alpha_e = 1 - \alpha_n + \alpha_p + Z_h \mu_h$, $\alpha_n = 1 - \alpha_e + \alpha_p + Z_h \mu_h$ and $\alpha_p = \alpha_n + \alpha_e - Z_h \mu_h - 1$. We have defined as $K_1 = n_{pi0}^{\alpha-1} K_i / m_e c^2$ and $K_2 = n_{e0}^{\gamma-1} K_e / m_e c^2 = n_{p0}^{\gamma-1} K_e / m_e c^2$.

3 Derivation of K -dV Equation

Now we derive a dynamical equation for the nonlinear propagation of the mIA solitary waves by using (7)–(12). To do so, we employ a reductive perturbation technique to examine electrostatic perturbations propagating in the relativistic degenerate dense plasma due to the effect of dispersion. We first introduce the stretched coordinates [32]:

$$\xi = -\epsilon^{1/2}(r + V_p t), \quad (13)$$

$$\tau = \epsilon^{3/2} t, \quad (14)$$

where V_p is the wave phase speed (ω/k with ω being angular frequency and k being the wave number of the perturbation mode), and ϵ is a smallness parameter measuring

the weakness of the dispersion ($0 < \epsilon < 1$). We then expand n_s , u_s , and ϕ in power series of ϵ :

$$n_s = 1 + \epsilon n_s^{(1)} + \epsilon^2 n_s^{(2)} + \dots, \quad (15)$$

$$u_s = \epsilon u_s^{(1)} + \epsilon^2 u_s^{(2)} + \dots, \quad (16)$$

$$\phi = \epsilon \phi^{(1)} + \epsilon^2 \phi^{(2)} + \dots, \quad (17)$$

and develop equations in various powers of ϵ . To the lowest order in ϵ , using (13)–(17) into (7)–(11), we get, $u_{pi}^{(1)} = V_p \phi^{(1)} / (V_p^2 - K_1')$, $u_{ni}^{(1)} = -\beta V_p \phi^{(1)} / (V_p^2 - K_1')$, $n_{pi}^{(1)} = \phi^{(1)} / (V_p^2 - K_1')$, $n_{ni}^{(1)} = -\beta \phi^{(1)} / (V_p^2 - K_1')$, $n_e^{(1)} = n_p^{(1)} = \phi^{(1)} / K_2'$, and $V_p = \sqrt{\frac{K_2' \{1 + \beta(1 - \alpha_e + \alpha_p + Z_h \mu_h)\}}{\{(1 - \alpha_n + \alpha_p + Z_h \mu_h) - (\alpha_n + \alpha_e - Z_h \mu_h - 1)\}}} + K_1'}$. The relation $V_p = \sqrt{\frac{K_2' \{1 + \beta(1 - \alpha_e + \alpha_p + Z_h \mu_h)\}}{\{(1 - \alpha_n + \alpha_p + Z_h \mu_h) - (\alpha_n + \alpha_e - Z_h \mu_h - 1)\}}} + K_1'}$ represents the dispersion relation for the mIA-type electrostatic waves in the degenerate plasma under consideration.

We are interested in studying the nonlinear propagation of these dispersive mIA-type electrostatic waves in a degenerate multispecies plasma. To the next higher order in ϵ , we obtain a set of equations:

$$\frac{\partial n_s^{(1)}}{\partial \tau} - V_p \frac{\partial n_s^{(2)}}{\partial \xi} + \frac{\partial}{\partial \xi} [u_s^{(2)} + n_s^{(1)} u_s^{(1)}] - \frac{v u_s^{(1)}}{V_p \tau} = 0, \quad (18)$$

$$\begin{aligned} \frac{\partial u_{pi}^{(1)}}{\partial \tau} - V_p \frac{\partial u_{pi}^{(2)}}{\partial \xi} + u_{pi}^{(1)} \frac{\partial u_{pi}^{(1)}}{\partial \xi} + \frac{\partial \phi^{(2)}}{\partial \xi} \\ + K_1' \frac{\partial}{\partial \xi} \left[n_{pi}^{(2)} + \frac{(\alpha - 2)}{2} (n_{pi}^{(1)})^2 \right] = 0, \end{aligned} \quad (19)$$

$$\begin{aligned} \frac{\partial u_{ni}^{(1)}}{\partial \tau} - V_p \frac{\partial u_{ni}^{(2)}}{\partial \xi} + u_{ni}^{(1)} \frac{\partial u_{ni}^{(1)}}{\partial \xi} - \beta \frac{\partial \phi^{(2)}}{\partial \xi} \\ + K_1' \frac{\partial}{\partial \xi} \left[n_{ni}^{(2)} + \frac{(\alpha - 2)}{2} (n_{ni}^{(1)})^2 \right] = 0, \end{aligned} \quad (20)$$

$$\frac{\partial \phi^{(2)}}{\partial \xi} - K_2' \frac{\partial}{\partial \xi} \left[n_e^{(2)} + \frac{(\gamma - 2)}{2} (n_e^{(1)})^2 \right] = 0, \quad (21)$$

$$\frac{\partial \phi^{(2)}}{\partial \xi} - K_2' \frac{\partial}{\partial \xi} \left[n_p^{(2)} + \frac{(\gamma - 2)}{2} (n_p^{(1)})^2 \right] = 0, \quad (22)$$

$$\frac{\partial^2 \phi^{(1)}}{\partial \xi^2} = \alpha_e n_e^{(2)} - n_{pi}^{(2)} + \alpha_n n_{ni}^{(2)} - \alpha_p n_p^{(2)}. \quad (23)$$

Now, combining (18)–(23), we deduce a K -dV equation

$$\frac{\partial \phi^{(1)}}{\partial \tau} + A \phi^{(1)} \frac{\partial \phi^{(1)}}{\partial \xi} + B \frac{\partial^3 \phi^{(1)}}{\partial \xi^3} + \frac{v \phi^{(1)}}{2\tau} = 0, \quad (24)$$

where the values of A and B are given by

$$A = \frac{(V_p^2 - K_1')^2}{2V_p(1 + \beta\alpha_n)} \left[\frac{(1 - \beta^2\alpha_n)(3V_p^2 + K_1'(\alpha - 2))}{(V_p^2 - K_1')^3} + \frac{(\gamma - 2)(\alpha_e - \alpha_p)}{K_2'^2} \right], \quad (25)$$

$$B = \frac{(V_p^2 - K_1')^2}{2V_p(1 + \beta\alpha_n)}. \quad (26)$$

4 Derivation of mK-dV Equation

Now we derive mK-dV equation by employing the reductive perturbation technique in order to examine the characteristics of the electrostatic solitary waves propagating in a dense plasma system for higher-order nonlinearity. We introduce the stretched coordinates [32] as follows:

$$\xi = -\epsilon(r + V_p t), \quad \tau = \epsilon^3 t. \quad (27)$$

By using (27) into (7)–(12) and taking the different order of ϵ , one can derive the following equation:

$$\frac{\partial \Phi^{(1)}}{\partial \tau} + \beta' \left\{ \Phi^{(1)} \right\}^2 \frac{\partial \Phi^{(1)}}{\partial \xi} + B \frac{\partial^3 \Phi^{(1)}}{\partial \xi^3} + \frac{\nu \Phi^{(1)}}{2\tau} = 0. \quad (28)$$

Equation (28) is known as mK-dV equation. Here, the value of B is as before and

$$\beta' = \alpha B \quad (29)$$

$$\alpha = \frac{15V_p^4 + 12K_1'V_p^2 + 18K_1'V_p^2(\alpha - 2) + 3K_1'(\alpha - 2)^2}{2(V_p^2 - K_1')^5} + \frac{K_1'(\alpha - 2)(\alpha - 3) - K_1'\alpha_n(\alpha - 2)(\alpha - 3)\beta^3}{2(V_p^2 - K_1')^4} + \frac{3K_1'^2\alpha_n(\alpha - 2)^2\beta^3 + 6\alpha_n\beta^3K_1'V_p^2(3\alpha - 4) + 15\alpha_n\beta^3V_p^4}{2(V_p^2 - K_1')^5} + \frac{(\alpha_e - \alpha_p)(4\gamma^2 - 11\gamma + 18)}{2K_2'^3}. \quad (30)$$

5 Numerical Analysis and Results

We now proceed with the presentation of our numerical results. We first briefly discuss the stationary solitary wave solution for (24). We should note that for a large value of τ , the term $\frac{\nu\phi^{(1)}}{2\tau}$ is negligible, i.e., $\frac{\nu\phi^{(1)}}{2\tau} \rightarrow 0$. So, in our numerical analysis, we start with a large value of τ (viz. $\tau = -14$), and at this large (negative) value of τ , we choose the stationary solitary wave solution of (24) [without the term $\frac{\nu\phi^{(1)}}{2\tau}$] as our initial pulse. The stationary solitary wave

solution of standard K-dV equation is obtained by considering a frame $\xi = \zeta - u_0\tau$ (moving with speed u_0) and the solution is

$$\phi_{(v \rightarrow 0)}^{(1)} = \phi_m \text{sech}^2\left(\frac{\xi}{\Delta}\right), \quad (31)$$

where the amplitude, $\phi_m = 3u_0/A$, and the width, $\Delta = (4B/u_0)^{1/2}$. Here, u_0 is the light ion fluid speed at equilibrium.

The stationary solitary wave solution of (28) is given by

$$\Phi_{(v \rightarrow 0)}^{(1)} = \Phi_m \text{sech}\left(\frac{\xi}{\delta}\right), \quad (32)$$

where the amplitude ϕ_m and the width δ_2 are given by $\Phi_m = \sqrt{6U_0/\alpha B}$ and $\delta = \Phi_m\sqrt{\gamma_1}$, $\gamma_1 = \alpha/6$.

Solitary waves often arise due to the balance between nonlinearity and dispersion, and their basic features are found to be significantly modified in the presence of nonrelativistic positively as well as negatively charged ions, both nonrelativistic and ultrarelativistic electron and positron fluids, and positively charged static heavy ions. The profiles are displayed in Figs. 4–19, which show how the effects of cylindrical ($\nu=1$) and spherical ($\nu=2$) geometries modify the time-dependent mIA solitary structures. We have considered $u_0 = 0.01$ for our numerical analysis of mIA waves for the multispecies plasma system under investigation here. We also considered that the ranges of the values of β , α_e , α_n , and α_p are 0.1 to 0.2, 0.1 to 0.25, 0.1 to 0.3, and 0.1 to 0.4, respectively [33–35]. In our numerical analysis, we first graphically represented the effects of $\mu_h (= n_{h0}/Z_{pi}n_{pi0})$ on the phase speed of mIA waves (as shown in Figs. 1, 2 and 3). Then we numerically solved (24) in case of cylindrical ($\nu = 1$) and spherical ($\nu = 2$) geometry on time dependent mIA solitary waves (as shown in Figs. 4, 5, 6, 7, 8, 9, 10, 11, 12, 13, 14, 15, 16, 17, 18, and 19). It is notable that if we compare the nonrelativistic (both electrons and

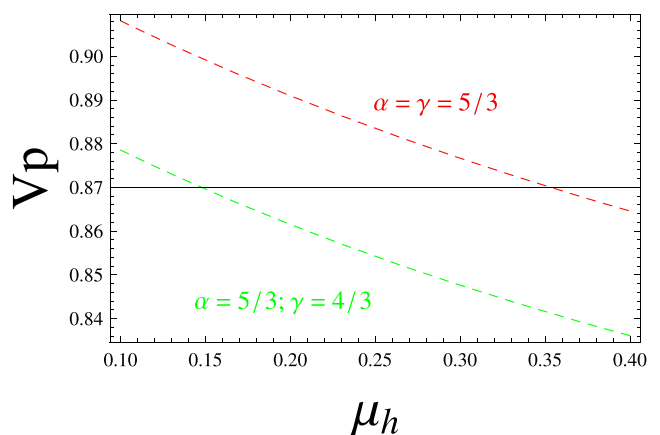


Fig. 1 (Color online) Variation of phase speed V_p with heavy ion-to-light ion number density ratio μ_h for $u_0 = 0.01$ and $Z_h = 1$. The dashed green line represents the ultrarelativistic case and the red one represents the nonrelativistic case

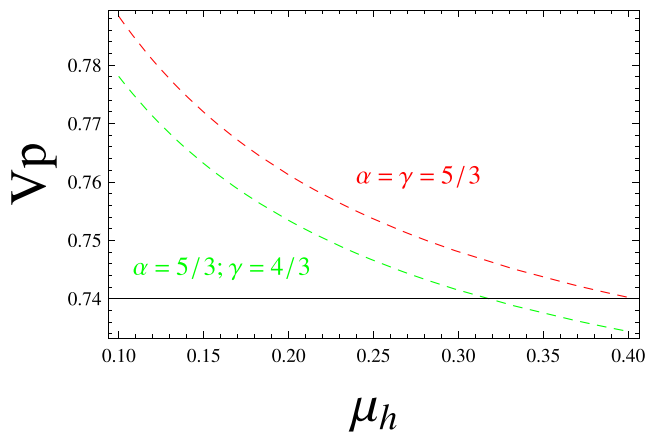


Fig. 2 (Color online) Variation of phase speed V_p with heavy ion-to-light ion number density ratio μ_h for $u_0 = 0.01$ and $Z_h = 5$. The dashed green line represents the ultrarelativistic case and the red one represents the nonrelativistic case

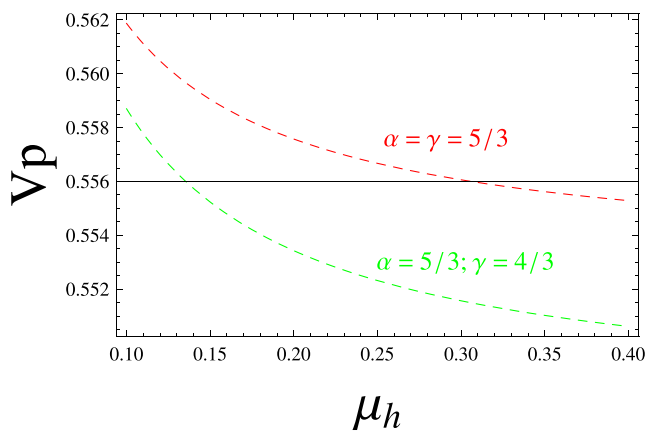


Fig. 3 (Color online) Variation of phase speed V_p with heavy ion-to-light ion number density ratio μ_h for $u_0 = 0.01$ and $Z_h = 100$. The dashed green line represents the relativistic case and the red one represents the nonrelativistic case

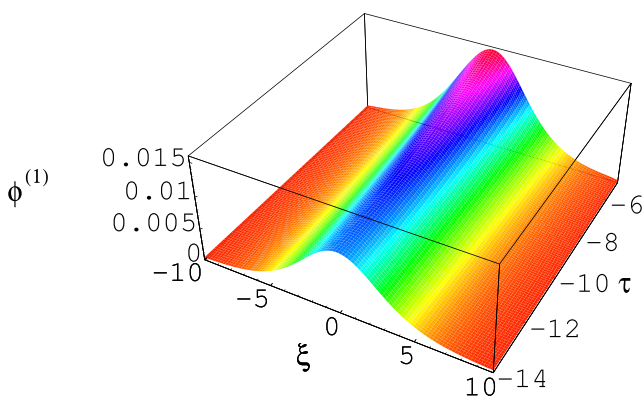


Fig. 4 (Color online) K-dV solitons in the presence of positively charged heavy ions and nonrelativistic degenerate electron, positron, and light ion fluids for $u_0 = 0.01$, $\nu = 1$, and $Z_h = 1$

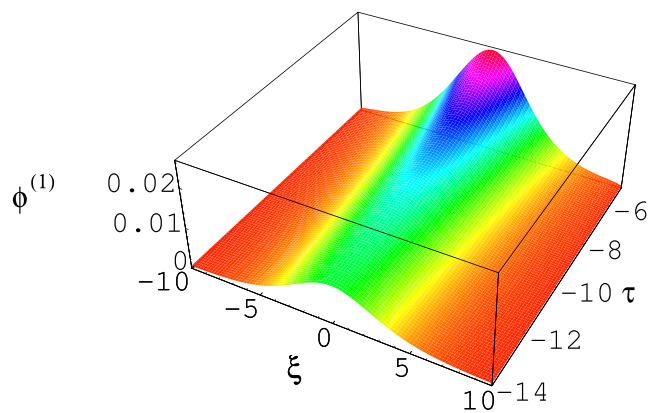


Fig. 5 (Color online) K-dV solitons in the presence of positively charged heavy ions and nonrelativistic degenerate electron, positron, and light ion fluids for $u_0 = 0.01$, $\nu = 2$, and $Z_h = 1$

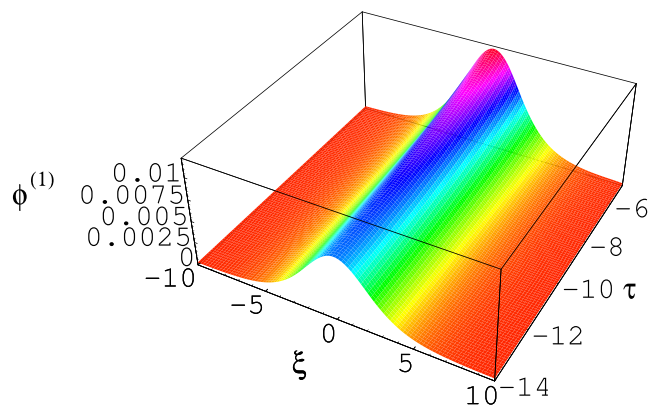


Fig. 6 (Color online) K-dV solitons in the presence of positively charged heavy ions, nonrelativistic degenerate light ions and ultrarelativistic degenerate electron and positron fluids for $u_0 = 0.01$, $\nu = 1$, and $Z_h = 1$

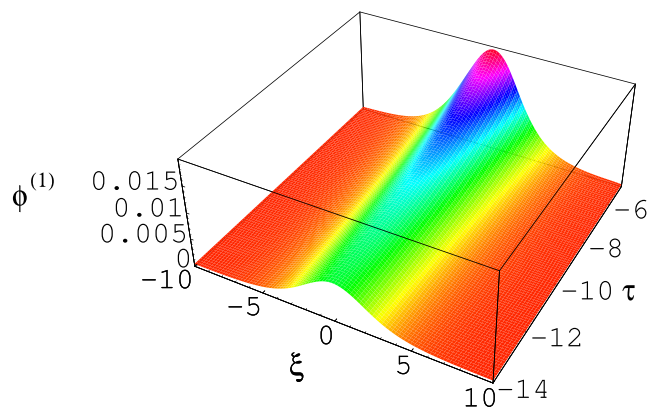


Fig. 7 (Color online) K-dV solitons in the presence of positively charged heavy ions, nonrelativistic degenerate light ions and ultrarelativistic degenerate electron and positron fluids for $u_0 = 0.01$, $\nu = 2$, $Z_h = 1$

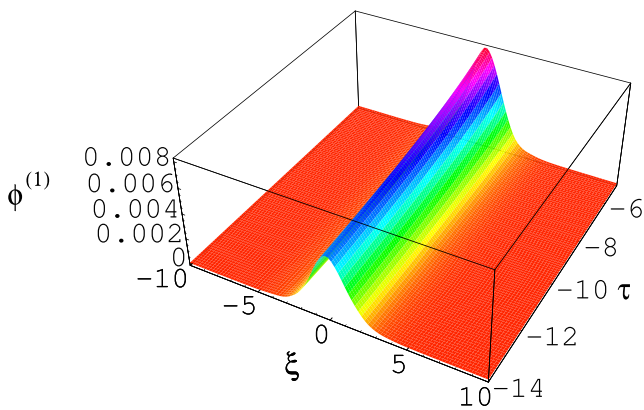


Fig. 8 (Color online) K-dV solitons in the presence of positively charged heavy ions and nonrelativistic degenerate electron, positron, and light ion fluids for $u_0 = 0.01$, $\nu = 1$, and $Z_h = 5$

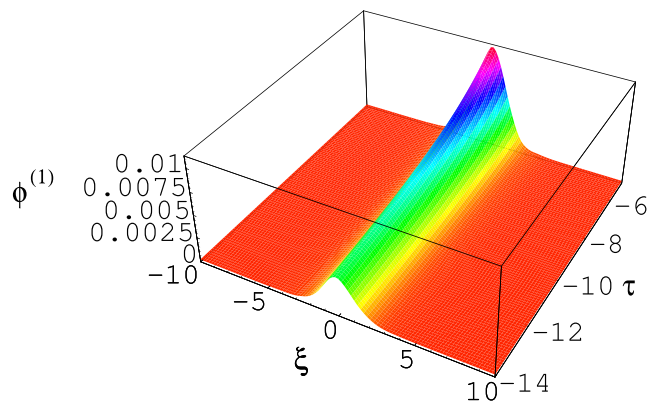


Fig. 11 (Color online) HIA solitary profile in the presence of positively charged heavy ions, nonrelativistic degenerate light ions and ultrarelativistic degenerate electron and positron fluids for $u_0 = 0.01$, $\nu = 2$, and $Z_h = 5$

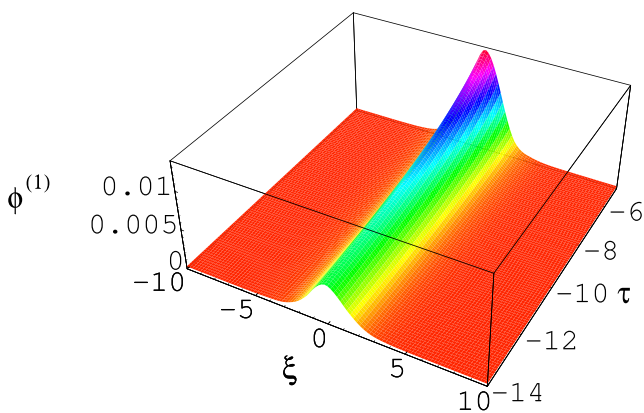


Fig. 9 (Color online) K-dV solitons in the presence of positively charged heavy ions and nonrelativistic degenerate electron, positron, and light ion fluids for $u_0 = 0.01$, $\nu = 2$, and $Z_h = 5$

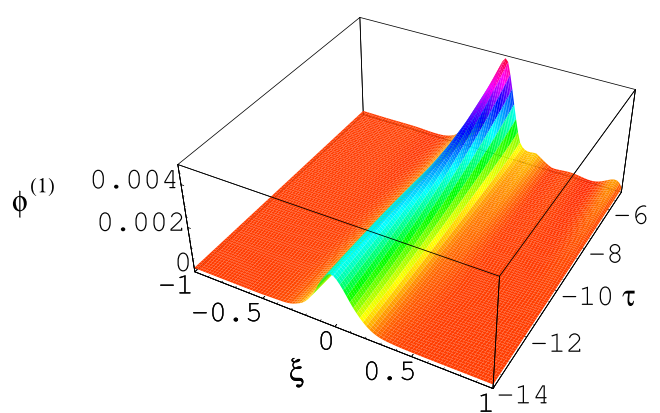


Fig. 12 (Color online) K-dV solitons in the presence of positively charged heavy ions and nonrelativistic degenerate electron, positron, and light ion fluids for $u_0 = 0.01$, $\nu = 1$, and $Z_h = 100$

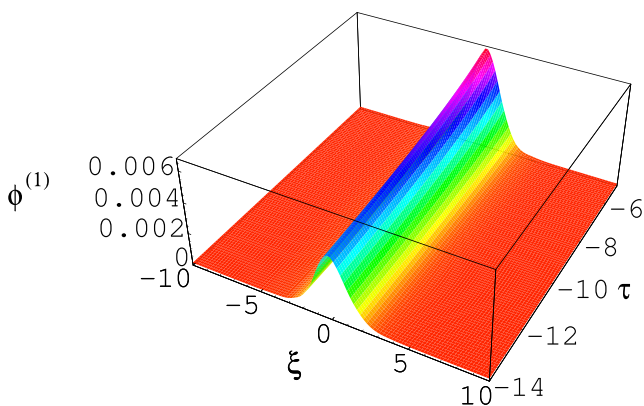


Fig. 10 (Color online) K-dV solitons in the presence of positively charged heavy ions, nonrelativistic degenerate light ions and ultrarelativistic degenerate electron and positron fluids for $u_0 = 0.01$, $\nu = 1$, and $Z_h = 5$

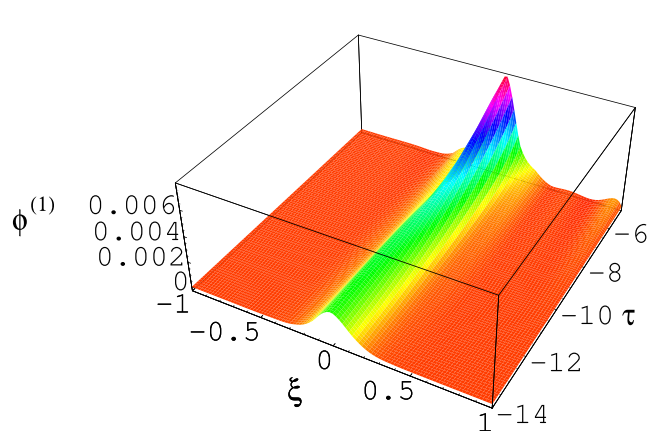


Fig. 13 (Color online) K-dV solitons in the presence of positively charged heavy ions and nonrelativistic degenerate electron, positron, and light ion fluids for $u_0 = 0.01$, $\nu = 2$, and $Z_h = 100$

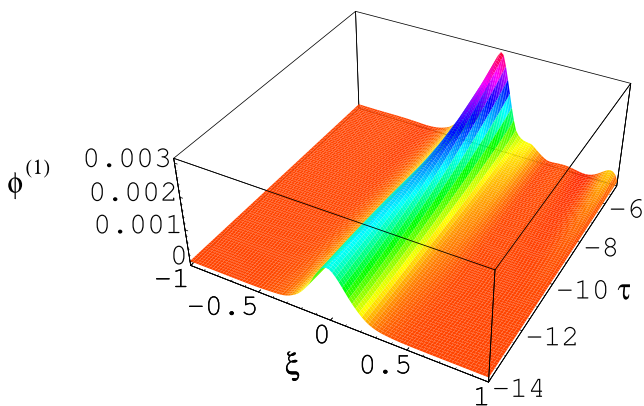


Fig. 14 (Color online) K-dV solitons in the presence of positively charged heavy ions, nonrelativistic degenerate light ions and ultrarelativistic degenerate electron and positron fluids for $u_0 = 0.01$, $\nu = 1$, and $Z_h = 100$

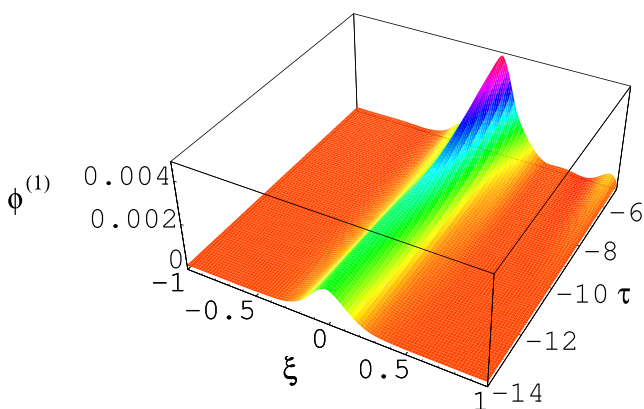


Fig. 15 (Color online) K-dV solitons in the presence of positively charged heavy ions, nonrelativistic degenerate light ions and ultrarelativistic degenerate electron and positron fluids for $u_0 = 0.01$, $\nu = 2$, and $Z_h = 100$

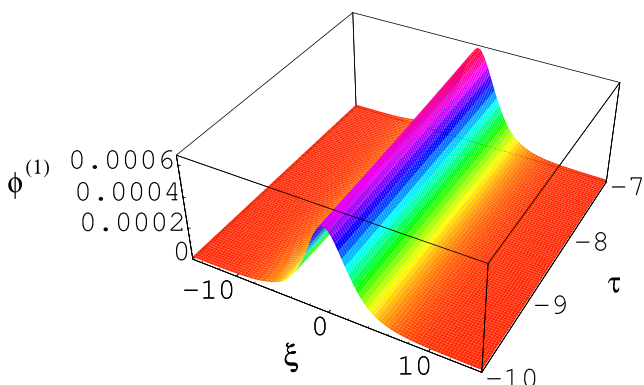


Fig. 16 (Color online) Showing the mK-dV solitons in the presence of positively charged heavy ions and nonrelativistic degenerate electron, positron, and light ion fluids for $u_0 = 0.01$, $\nu = 1$, and $Z_h = 1$

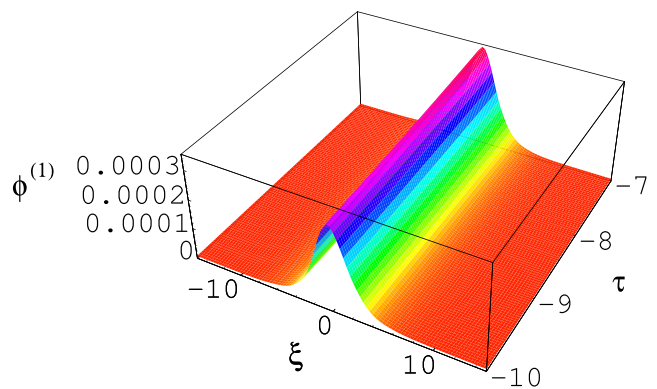


Fig. 17 (Color online) Showing the mK-dV solitons in the presence of positively charged heavy ions, nonrelativistic degenerate light ions and ultrarelativistic degenerate electron and positron fluids for $u_0 = 0.01$, $\nu = 1$, and $Z_h = 1$

ions are nonrelativistic degenerate) and ultrarelativistic case (electrons are ultrarelativistic degenerate and ions are nonrelativistic degenerate) for mIA waves, one cylindrical and one spherical solitary structure will be found for every case (see Figs. 4–19).

Figures 1–3 show the variation of phase speed (V_p) with heavy ion to light ion number density ratio μ_h . It is found that the phase speed decreases with the increasing values of μ_h . This is expected, as the phase velocity V_p (derived from this considered plasma) is higher for lower values of μ_h (see the expression of V_p in Section 3). Figures 4–19 show the time evolution of solitary structures in cylindrical and spherical geometry. We have found that as time decreases, the amplitude of the solitary waves in cylindrical and spherical geometry increases. It is also examined that in spherical geometries, the amplitude is always distinctly higher than cylindrical geometries for both K-dV and mK-dV solitons, which indicate that the density compression can be more effectively obtained in a spherical

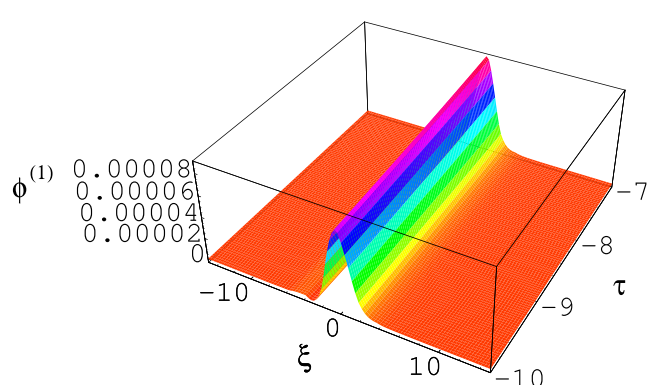


Fig. 18 (Color online) Showing the mK-dV solitons in the presence of positively charged heavy ions and nonrelativistic degenerate electron, positron, and light ion fluids for $u_0 = 0.01$, $\nu = 1$, and $Z_h = 5$

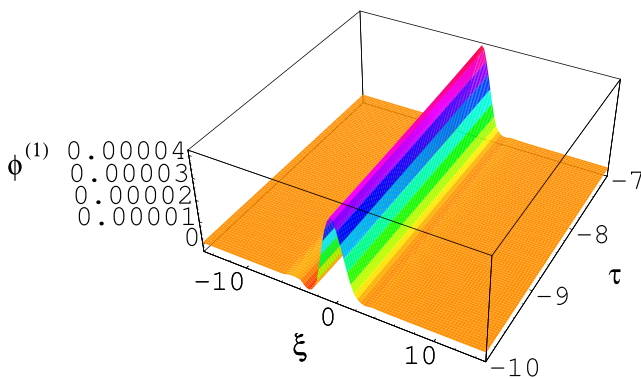


Fig. 19 (Color online) Showing the mK-dV solitons in the presence of positively charged heavy ions, nonrelativistic degenerate light ions and ultrarelativistic degenerate electron and positron fluids for $u_0 = 0.01$, $\nu = 1$, and $Z_h = 5$

geometry. Finally, the results that we have found in this investigation can be summarized as follows:

1. The plasma system under consideration supports mIA K-dV and mK-dV solitons whose basic characteristics (speed, amplitude, and width) are found to be significantly modified due to the various charging states of positively charged static heavy ions.
2. The phase speed of the mIA waves decreases with the increase of the value of μ_h . It is obvious from Figs. 1–3 as the value of Z_h ($Z_h = 1, 5, 100$) increases, the phase speed slowly decreases for both nonrelativistic and ultrarelativistic cases in the presence of positively charged static heavy ions.
3. The amplitude of the mIA waves is found to decrease with the increasing values of heavy ion charge state Z_h (see Figs. 4–19).
4. The large value of τ kills the possibility of the formation of nonplanar solitary waves. It is found that as the value of τ decreases, the amplitude of these localized pulses increases for mIA waves (see Figs. 4–19).
5. It is found from Figs. 4–19 that the amplitude is lower for ultrarelativistic case than for nonrelativistic case for both cylindrical ($\nu = 1$) and spherical ($\nu = 2$) geometries.
6. If we compare the $\nu = 1$ graphs with the $\nu = 2$ ones, we observe that the amplitude is always distinctly higher for $\nu = 2$ case than $\nu = 1$ case for mIA waves (see Figs. 4–19).
7. It is observed that the inclusion of higher-order nonlinearity (assumed via modified K-dV) significantly influenced the basic features of solitary waves. For example, the amplitude of mK-dV solitons is seen to lower in comparison to K-dV solitons for both nonrelativistic and ultrarelativistic limits (see Figs. 4–19).

6 Discussion

To conclude, we have presented a rigorous theoretical investigation of the nonlinear propagation of mIA solitary waves in an unmagnetized, collisionless dense plasma (containing degenerate electron and positron fluids, inertial positively as well as negatively charged light ions, and positively charged static heavy ions). The positively charged static heavy ions participate only in maintaining the quasi-neutrality condition at equilibrium. It is found that as time increases the value of the amplitude of cylindrical and spherical mIA, solitary wave height decreases. The basic features (speed, amplitude, and width) of mIA solitary waves are found to be significantly modified due to the various charging situations of positively charged static heavy ions ($Z_h = 1, 5, 100$), and the number densities of the degenerate electron and positron fluids, and nondegenerate positively as well as negatively charged ions. It is found that the amplitude of the solitary waves has been modified by the heavy ion number density (via μ_h). We have studied the effect of nonplanar (cylindrical and spherical) geometry on the propagation of mIA solitary waves, where degenerate plasma pressure and positively charged static heavy ions are accountable. This model is also precisely/rigorously valid for a large value of Z_h ($Z_h > 100$). Our results that we have investigated in this paper should be useful to understand the solitary wave properties [24, 36, 37] in matter under extreme conditions, e.g., interior of compact objects (where positively charged static heavy ions, inertial positively as well as negatively charged light ions, and degenerate plasma pressure are accountable). This theory could also be important for global nonlinear and nonplanar models of astrophysical compact objects like nonrotating white dwarfs, neutron stars etc.

References

1. H.R. Miller, P.J. Witta, *Active Galactic Nuclei* (Springer, Berlin, 1987)
2. J.M. Wang, Ph. Durouchoux, T.P. Li, *Astrophys. Space Sci.* **276**, 301 (2011)
3. P. Helander, D.J. Ward, *Phys. Rev. Lett.* **90**, 135004 (2003)
4. O. Adrani, G.C. Barbarino, G.A. Bazilevskaya et al., *Nature* **458**, 607 (2009)
5. C.M. Surko, T.J. Murphy, *Phys. Fluids B* **2**, 1372 (1990)
6. D. Lai, *Rev. Mod. Phys.* **73**, 629 (2001)
7. A.K. Harding, D. Lai, *Rep. Prog. Phys.* **69**, 2631 (2006)
8. S.L. Shapiro, S.A. Teukolsky, *Black Holes, White Dwarfs and Neutron Stars: The Physics of Compact Objects* (John Wiley Sons, New York) (1983)
9. R.A. Gottscho, C.E. Gaebe, *IEEE Trans. Plasma Sci.* **14**, 92 (1986)
10. M. Bacal, G.W. Hamilton, *Phys. Rev. Lett.* **42**, 1538 (1979)
11. J. Jacquiot, B.D. McVey, J.E. Scharer, *Phys. Rev. Lett.* **39**, 88 (1977)
12. D.E. Shemansky, D.T. Hall, *J. Geophys. Res.* **97**, 4143 (1992)

13. B. Hultqvist, M. Ieroset, G. Paschmann, R. Treumann, *Magnetospheric Plasma Sources and Losses* (Kluwer Academic, Dordrecht, 1999)
14. K. Stasiewicz, Phys. Rev. Lett. **12**, 125004 (2004)
15. H. Massey, *Negative Ions* (Cambridge University Press, Cambridge, 1976)
16. P.H. Chaizy et al., Nature **349**, 393 (1991)
17. S. Chandrasekhar, Phi. Mag. **11**, 592 (1931)
18. S. Chandrasekhar, Astrophys. J. **74**, 81 (1931)
19. S. Chandrasekhar, Mon. Not. R. Astron. Soc. **170**, 405 (1935)
20. M.R. Hossen, L. Nahar, S. Sultana, A.A. Mamun, High Energ. Density Phys. (2014). doi:[10.1016/j.hedp.2014.08.001](https://doi.org/10.1016/j.hedp.2014.08.001)
21. S. Chandrasekhar, *An Introduction to the Study of stellar structure* (Dover Publications, New York, 1939)
22. G.B. Van Albada, Astrophys. J. **105**, 393 (1947)
23. A.A. Mamun, P.K. Shukla, Phys. Lett. A **324**, 4238 (2010)
24. A.A. Mamun, P.K. Shukla, Phys. Plasmas **17**, 104504 (2010)
25. M.R. Hossen, L. Nahar, S. Sultana, A.A. Mamun, Astrophys. Space Sci. **353**, 123 (2014)
26. S.A. Khan, A.M. Mirza, Commun. Theor. Phys. **55**, 151 (2011)
27. L. Gaimin, Y. Liu, S. Zheng, Y.M. Wang, W. Yu, M.Y. Yu, Astrophys. Space Sci. **330**, 73 (2010)
28. I. Zeba, W.M. Moslem, P.K. Shukla, Astrophys. J. **750**, 6 (2012)
29. N. Roy, S. Tasnim, A.A. Mamun, Phys. Plasmas **19**, 033705 (2012)
30. M.S. Zobaer, K.N. Mukta, A.A. Mamun, Int. J. Sci. Eng. Res. **4**, 8 (2013a)
31. K.N. Mukta, M.S. Zobaer, N. Roy, A.A. Mamun, J. Plasma Phys. (2013). doi:[10.1017/S0022377813000032](https://doi.org/10.1017/S0022377813000032)
32. S. Maxon, J. Vieceilli, Phys. Rev. Lett. **32**, 4 (1974)
33. M.S. Zobaer, L. Nahar, A.A. Mamun, IJERT **2**, 1 (2013)
34. M.R. Hossen, L. Nahar, A.A. Mamun, Braz. J. Phys. (2014). doi:[10.1007/s13538-014-0242-6](https://doi.org/10.1007/s13538-014-0242-6)
35. T. Akhter, M.M. Hossain, A.A. Mamun, Commun. Theor. Phys. **59**, 745 (2013)
36. W. Masood, B. Eliasson, Phys. Plasmas **18**, 034503 (2011)
37. Ata-ur-Rahman, S. Mustaq, A. Ali, Commun. Qamar. Theor. Phys. **59**, 479 (2013)